2017

# Five-Year Longitudinal Brain Volume Change in Healthy Elders at Genetic Risk for Alzheimer's Disease

Katherine Reiter
*Marquette University*

Kristy A. Nielson
*Marquette University*, kristy.nielson@marquette.edu

Sally Durgerian
*Medical College of Wisconsin*

John L. Woodard
*Wayne State University*

J. Carson Smith
*University Of Maryland College Park*

*See next page for additional authors*

Authors

Katherine Reiter, Kristy A. Nielson, Sally Durgerian, John L. Woodard, J. Carson Smith, Michael Seidenberg, Dana A. Kelly, and Stephen M. Rao

# Five-Year Longitudinal Brain Volume Change in Healthy Elders At Genetic Risk for Alzheimer's Disease

## Katherine Reiter

*Department of Psychology, Marquette University*
*Milwaukee, WI*

## Kristy A. Nielson

*Department of Psychology, Marquette University,*
*Department of Neurology, Medical College of Wisconsin*
*Milwaukee, WI*

## Sally Durgerian

*Department of Neurology, Medical College of Wisconsin*
*Milwaukee, WI*

## John L. Woodard

*Department of Psychology, Wayne State University*
*Detroit, MI*

# J. Carson Smith

*Department of Kinesiology, School of Public Health, University of Maryland*
*College Park, MD*

# Michael Seidenberg

*Department of Psychology, Rosalind Franklin University,*
*North Chicago, IL*

# Dana A. Kelly

*Department of Psychology, Rosalind Franklin University,*
*North Chicago, IL*

# Stephen M. Rao*

*Schey Center for Cognitive Neuroimaging,*
*Lou Ruvo Center for Brain Health,*
*Neurological Institute, Cleveland Clinic*
*Cleveland, OH*

**Abstract:** Neuropathological changes associated with Alzheimer's disease (AD) precede symptom onset by more than a decade. Possession of an Apolipoprotein-E (*APOE*) ε4 allele is the strongest genetic risk factor for late onset AD. Cross-sectional studies of cognitively intact elders have noted smaller hippocampal/medial temporal volumes in ε4 carriers (ε4+) compared to ε4 non-carriers (ε4-). Few studies, however, have examined long-term, longitudinal, anatomical brain changes comparing healthy ε4+ and ε4- individuals. The current five-year study examined global and regional volumes of cortical and subcortical grey and white matter and ventricular size in 42 ε4+ and 30 ε4- individuals. Cognitively intact participants, ages 65-85 at study entry, underwent repeat anatomical MRI scans on three occasions: baseline, 1.5, and 4.75 years. Results indicated no between group volumetric differences at baseline. Over the follow-up interval, the ε4+ group experienced a greater rate of volume loss in total grey matter, bilateral hippocampi, right hippocampal subfields, bilateral lingual gyri, parahippocampal gyrus, and right lateral orbofrontal cortex compared to the ε4- group. Greater loss in grey matter volumes in ε4+ participants were accompanied by greater increases in lateral, third and fourth ventricular volumes. Rate of change in white matter volumes did not differentiate the groups. The current results indicate that longitudinal measurements of brain atrophy can serve as a sensitive biomarker for identifying neuropathological

changes in persons at genetic risk for AD and potentially, for assessing the efficacy of treatments designed to slow or prevent disease progression during the preclinical stage of AD.

**Keywords:** Longitudinal Studies, MRI Scans, Alzheimer Disease, ApoE4

# Introduction

The neuropathological changes associated with Alzheimer's disease (AD) may occur decades prior to the onset of clinical symptoms.[1] Identification of individuals in the preclinical stage of AD is essential to developing successful interventions designed to prevent or slow down the neuropathological processes leading to cognitive decline and dementia. In addition to advancing age and a family history of dementia,[2] the ε4 allele of the Apolipoprotein-E (*APOE*) gene is a well-recognized AD risk factor.[3] Possession of the ε4 allele is associated with a greater rate of hippocampal and medial temporal lobe atrophy in patients diagnosed with Mild Cognitive Impairment (MCI) and AD.[4,5] Conceivably, a greater rate of hippocampal and medial temporal lobe atrophy could also be used to identify persons during the preclinical stage of AD. One approach would involve the longitudinal study of brain atrophy comparing cognitively intact elders possessing one or both ε4 alleles with similarly aged non-carriers.

Longitudinal studies of brain atrophy comparing ε4 carriers and non-carriers show mixed results (see Table 1). Most of these studies focus on the hippocampus, due to its known relationship with early AD pathogenesis.[6] Some longitudinal studies have demonstrated that cognitively intact elders possessing the ε4 allele experience greater hippocampal atrophy over time compared to non-carriers,[7-9] although these results have not been demonstrated in other studies.[10-12] Notably, most of these studies measured the rate of atrophy based on two MRI assessments.

Only a few studies in Table 1 examined longitudinal changes in brain regions outside the medial temporal lobes. A measure of total brain volume demonstrated a greater rate of atrophy in ε4 carriers than non-carriers.[8] In one study, total grey matter volume atrophied at a faster rate in ε4 homozygotes relative to ε4 heterozygotes and non-carriers.[13] Healthy ε4 carriers also experienced a greater rate of

volume loss in the temporal lobes compared to non-carriers.[14] No study has yet reported comprehensive rates of change in global and regional volumes comprising the entire brain.

The current study, therefore, evaluated the influence of the ε4 allele on brain volume changes in cognitively intact elders who underwent repeat cognitive testing and anatomical MRI at study entry and after 1.5 and 4.75 years. The three scan sessions enable a more precise examination of the slope of volume change over time. The MRI volumetric analysis, based on Freesurfer software, enabled a comprehensive examination of global and regional grey and white matter volumes and ventricular size, as well as specific examination of the hippocampus and hippocampal subfields. We employed a longitudinal linear mixed-effects (LME) analysis that permitted modeling of the precise time intervals between assessments as well as allowance for missing observations. We predicted that ε4 carriers would exhibit greater atrophy than non-carriers in the hippocampus and other cortical regions that are particularly vulnerable to AD pathogenesis, such as the medial temporal[4] and frontal regions.[15]

## Materials and Methods

### Participants

The recruitment strategy for this study, described in detail in Seidenberg, et al.,[16] involved over-sampling persons at genetic risk for AD based on the presence of an *APOE* ε4 allele. Briefly, healthy older adults between the ages of 65 and 85 were recruited from newspaper advertisements. Screening via telephone of 459 individuals was conducted for willingness to participate and to exclude participants based on: MRI scanning criteria (e.g., weight inappropriate for height, ferrous objects within the body, history of claustrophobia); non-right handedness; depression [Geriatric Depression Scale (GDS)[17] score > 20]; impaired activities of daily living [Lawton Instrumental Activities of Daily Living (IADL)[18] scale < 5]; current use of psychoactive medications; and history of major neurological, medical, or psychiatric (DSM-IV Axis-I criteria) diseases or disorders. All procedures were approved by the Institutional Review Board of the Medical College of Wisconsin, which had oversight of this study. Written informed consent

was obtained from all participants and they received financial compensation for their participation.

Of those meeting eligibility criteria, 109 agreed to undergo *APOE* genotype testing from blood samples, a neuropsychological evaluation, and an MRI scanning session. APOE genotype was determined using a polymerase chain reaction method. DNA was isolated with Gentra Systems Autopure LS for Large Sample Nucleic Acid Purification.[19] We excluded 31 ε4- participants who had a family history (FH) of AD to isolate APOE as the primary AD genetic risk factor. FH was defined as a reported first degree relative with a history of gradual decline in memory and other cognitive domains, and confusion. Of the remaining 78 participants, only those with a minimum of two technically adequate MRI scans were included in the final sample. Six participants were excluded because they had only baseline data: withdrawal from study (3), scan failure/refusal (2), and lost to followup (1).

The final sample consisted of 72 participants divided into two groups: 1) the *APOE* ε4 positive group (ε4+; n=42), who were carriers of one or both ε4 alleles (ε2/ε4: 1; ε3/ε4: 39; ε4/ε4: 2); and 2) the ε4 negative group (ε4-; n=30), (ε2/ε3: 2; ε3/ε3: 28). Table 2 shows the baseline characteristics of the ε4+ and ε4- groups. No significant group differences were observed for age or sex. A non-significant trend was observed for education, with a mean 1.3 years of greater attainment observed in the ε4+ than ε4- group; as a result, all subsequent analyses employed education as a covariate. Two-thirds of the ε4+ group had a FH of AD, whereas none of the ε4- group had a FH. None of the participants had clinical levels of depression (GDS) or problems with activities of daily living.

Mean follow-up intervals for the ε4+ participants were 1.5 years (SD = 0.1) and 4.7 years (SD = 0.4). For the ε4- participants, the follow-up intervals were 1.5 years (SD = 0.2) and 5.0 years (SD = 0.5). No significant group differences were observed. Three participants (all ε4+) had baseline and second follow-up scans, but no first follow-up scan; 21 participants (12 ε4+; 9 ε4-) completed baseline and first follow-up scans, but were unable to be scanned at the second follow-up due to: health decline (6), deceased (5), lost

to follow-up (3), refused scan (3), moved away (3), and no longer safe to be scanned (1). No group differences were observed in attrition rates at each of the two follow-up scan sessions.

## Procedure

For each session, neuropsychological testing and MRI were conducted on the same day. Participants were asked to refrain from alcohol use for 24 h and caffeine use 12 h prior to testing. The neuropsychological test battery consisted of the Mini Mental State Examination (MMSE) [20], Mattis Dementia Rating Scale 2 (DRS-2),[21] and Rey Auditory Verbal Learning Test (RAVLT).[22]

## MRI Acquisition and Processing

High-resolution, three-dimensional spoiled gradient-recalled at steady-state (SPGR) anatomic images were acquired on a General Electric (Waukesha, WI) Signa Excite 3.0 Tesla short bore scanner equipped with a quad split quadrature transmit/receive head coil (TE = 3.9 ms; TR = 9.5 ms; inversion recovery (IR) preparation time = 450 ms; flip angle = 12°; number of excitations (NEX) = 2; slice thickness = 1.0 mm; FOV = 24 cm; resolution = 256 × 224). A scanner upgrade took place near the end of the final retest period. Six ε4+ participants and one ε4- had their third scan conducted on a GE MR750 3.0 Tesla scanner (TE = 3.9 ms; TR = 9.6 ms; inversion recovery (IR) preparation time = 450 ms; flip angle = 12°; number of excitations (NEX)=1; slice thickness = 1.0 mm; FOV = 24 cm; resolution=256×224). A between-scanner comparison showed no systematic differences. Whole brain and regional volumes were derived from T1- weighted SPGR images using the longitudinal stream in Freesurfer v.5.1 software.[23]

## Statistical analysis

All data were analyzed using R software, version 3.2.2. A longitudinal LME analysis was used to model the effects of genetic risk and time on anatomical volumes, with baseline age, education and intracranial volume included as covariates. LME permits an unequal number of within-subject observations, making this technique flexible

in cases where missing data may occur. The level-one random effects model was linear within-subject volume as a function of time at baseline and was used to assess volume differences at baseline between carrier groups. Time was flexibly expressed as fractional number of years since baseline for each observation in each subject.

The level-two fixed effects model estimated group differences in the slope of volume change with years post baseline as the measure of time. The non-carrier (ε4-) group provided the base (i.e., reference) model; differences in rate of atrophy of the carrier (ε4+) group were modeled with respect to the ε4- group. Thus, a statistically significant slope in the non-carrier group is reflected by a rate of change greater than 0 (data column 3 in Tables 3-7). A statistically significant group difference (carrier vs. non-carrier) in slope is shown in data column 4 of Tables 3-7. A statistically significant slope in the non-carrier group (data column 3), but a non-significant slope difference between the carrier and non-carrier groups (data column 4), indicates that the rate of change in both groups is comparable (i.e., normal aging effect).

The level-two model included nuisance variables as covariates, including baseline age, intracranial volume and education. Residuals were visually inspected using quantile–quantile plots to confirm the assumption of normality. Coefficients, standard errors, t-statistics and associated p-values were tabulated for each region. False discovery rate was applied to correct for multiple comparisons; this correction was applied separately to different classes of data (e.g., white matter vs. grey matter volumes). Statistically significant negative slopes in the ε4- group represent atrophy as a function of time that is comparable in both carriers and non-carriers. Statistically significant negative slopes in the ε4+ vs. ε4- groups represent greater rates of atrophy in ε4 carriers. Thus, regions that show greater rates of atrophy in ε4 carriers compared to non-carriers represent atrophy specific to the ε4 allele.

# Results

## *Baseline Cognitive Functioning*

No significant group differences were observed on the MMSE, the total score and subscales of the DRS-2, or the RAVLT; these measures were well within the normal ranges.

## *LME Analyses*

A quadratic model was also considered, but comparison of the Akaike Information Criterion (AIC) for each model indicated that the linear model was preferred. Table 3 summarizes results of the LME analyses applied to the total left and right hippocampal volumes and parcellated hippocampal subfields. No significant group differences were observed at baseline (intercept) between the ε4- and ε4+ groups. No differences over time (slope) were observed in the ε4- group. In contrast, the ε4+ group showed significantly greater rates of change than the ε4- group in the left and right hippocampi (see top panel of Figure 1) and multiple right sided hippocampal subfields: Cornu Ammonis (CA)2/3, CA4/DG, presubiculum, and subiculum (changes in CA2/3 and CA4/DG are shown in the middle panel of Figure 1).

Table 4 summarizes results of whole brain cortical grey matter (GM), white matter (WM), and ventricular volumes. No baseline group differences were observed. Over time, both groups showed significantly decreased volume in the right and left cortical WM and increased volume within the right and left lateral, inferior lateral, third, and fourth ventricles. The ε4+ group showed statistically greater rates of atrophy in bilateral cortical GM and greater increases in volume of the lateral, inferior lateral, and third ventricles compared to the ε4- group. Longitudinal changes in the left and right lateral ventricles are shown in the bottom panel of Figure 1.

Tables 5 and 6 summarize right and left cortical GM volumes, respectively. No baseline group differences were observed. Decreased volume of the right transverse temporal cortex and the left middle

temporal, pars orbitalis, and superior temporal gyrus were observed in the ε4- group over time. The ε4- group also showed increased volume in left lingual gyrus over time. Compared to the ε4- group, the ε4+ group had a greater rate of atrophy within the lingual and parahippocampal gyri (PHG) and right lateral orbitofrontal cortex (OFC).

Tables 7 and 8 summarize right and left cortical WM volumes, respectively. No significant group differences were observed at baseline. The ε4- group experienced reduced volumes over time in 19 bilateral WM regions, six unique regions within the right hemisphere, and 1 within the left hemisphere. Notably, the rate of decline in WM regions did not differ between the ε4+ and ε4- groups.

Table 9 summarizes results of subcortical volumetric analyses. No significant between group differences were observed at baseline. Over time, the ε4- group had reduced volumes in the right and left putamen, left accumbens, and left amygdala. No differences were observed in the rate of change in volume over time between the ε4+ and ε4- groups.

## Discussion

Our cognitively intact and healthy ε4 carriers and non-carriers, who were enrolled between the ages of 65 and 85, did not demonstrate any brain volumetric differences at study entry. Over the course of the five-year follow-up interval, the rate of brain atrophy was significantly greater in the carriers than in the non-carriers. Consistent with prior investigations (see Table 1), we observed greater shrinkage of the hippocampi in carriers than non-carriers. When examining hippocampal subfields, we observed shrinkage primarily of the CA2,3, CA4-DG, presubiculum and subiculum regions in the right hemisphere. The greater atrophy seen in carriers relative to non-carriers is not confined to the hippocampus, but extends to the lingual and parahippocampal regions, as well as the lateral orbitofrontal cortex. Carriers also experienced global atrophic changes over time, with greater reductions in total cortical GM and increases in the lateral and third ventricles, compared to non-carriers. Finally, while longitudinal reductions in total and regional WM volumes were

prominent as part of the aging process, no differences in the rate of WM atrophy were observed between carriers and non-carriers.

These findings suggest that possession of the *APOE* ε4 allele is associated with more accelerated brain atrophy rates in healthy elders, suggesting that some of the carriers may be experiencing the effects of underlying AD-related neuropathology. Although we do not have independent confirmation that the greater rates of atrophy in our carriers are linked to AD neuropathology (i.e., evidence of amyloid-β or tau from CSF or PET scans), we[9] have previously reported that a significantly higher percentage of our carrier group converted to a diagnosis of MCI at the five year follow-up examination compared to our non-carrier group. In the current sample, which overlaps but is not identical to our previously published study,[9] 12 of 72 participants (16.7%) met MCI criteria within the 5- year study period. Of these participants, 10 were carriers and two were non-carriers. Thus, 10 of 42 (23.8%) carriers, but only 2 of 30 (6.7%) non-carriers, converted to MCI. Given this association and the relatively small overall number of MCI converters, it is not possible to examine the separate influence of MCI conversion and carrier status on regional brain atrophy rates.

The precise mechanisms that link AD pathogenesis with the *APOE* ε4 allele are not well understood. The *APOE* gene is related to cholesterol metabolism and axonal repair after injury. The *APOE* ε4 allele negatively influences synaptic functioning and dendritic branching.[24] Other studies have suggested that ε4 confers a greater risk to developing AD through inhibiting amyloid-β (Aβ) clearance.[25,26] Aβ detected in healthy elders has been associated with neural degeneration[27] and specifically with hippocampal atrophy.[28] The current working hypothesis suggests that abnormal processing of Aβ peptides and associated formation of Aβ plaques precede neurodegenerative changes (i.e., atrophy) and cognitive dysfunction.[1]

Our results confirm previous research indicating that the most profound and earliest AD-related atrophic changes are observed within the hippocampal region. Hippocampal volume loss tracks AD disease progression, with MCI patients showing greater hippocampal atrophy compared to healthy elders and AD patients showing more pronounced hippocampal atrophy than MCI patients.[29] Our study extended

previous investigations by examining volumetric rates of change in hippocampal subfields. Our carriers demonstrated greater rates of atrophy in CA2/3, CA4/dentate gyrus, presubiculum, and subiculum layers (right hemisphere), whereas the CA1, fimbria, and hippocampal fissure were not affected. Interestingly, although both the right and left total hippocampal volumes showed greater rates of atrophy in carriers compared to noncarriers, and both right and left hippocampal subfields showed greater atrophy in the carriers than non-carriers, only group differences in the right hippocampal subfields survived FDR correction. This outcome may reflect statistical factors, such as sample size and measurement variability, rather than true asymmetric rates of atrophy within the subfields. Cross-sectional studies have demonstrated smaller CA3 and dentate gyri[30] and subiculum4 in healthy elders with the ε4 allele. Furthermore, CA[1] and subicular atrophy has been shown to predict conversion from normal aging to amnestic MCI over 6 years in a study that did not consider *APOE* genotype.[31]

Our study found a greater rate of ventricular dilatation in carriers relative to noncarriers. This increased rate of enlargement occurred primarily within the lateral and third ventricles, with the fourth ventricle being spared. Although we did not observe baseline differences in ventricular volumes between carriers and non-carriers, a cross sectional study reported greater ventricular volumes in healthy older ε4 carriers relative to age matched non-carriers.[32] Greater longitudinal rates of change in lateral ventricular size are common in AD, with rates of change in MCI and AD patients significantly greater than in healthy elders.[33] CSF measures of Aβ have been associated with greater ventricular enlargement over time in healthy elders, especially in ε4 carriers.[34]

Only one prior study[13] has examined total GM atrophy in a 3.6-year longitudinal study of elderly ε4 carriers. They observed a greater total cortical GM atrophy rate in ε4 homozygotes than in ε4 heterozygotes and non-carriers using voxel based morphology (VBM). In contrast to our study in which 95% of the carriers were heterozygotes, no differences in GM atrophy rates were observed between heterozygotes and non-carriers. These conflicting findings

may be related to possible methodological differences between VBM and Freesurfer in calculating bran volumes.

Carriers exhibited greater atrophy in bilateral lingual and parahippocampal gyri and in right lateral orbitofrontal cortex. The lingual and parahippocampal gyri appear to be particularly vulnerable to AD-related neuropathology. Specifically, reduced cerebral metabolic rates have been reported in these regions for ε4 carriers vs. non-carriers,[35] and atrophy in these regions predicts conversion from MCI to AD.[36] Similarly, orbitofrontal cortex volume has been shown to distinguish healthy elders from those with MCI and AD.[37] Better lateral orbitofrontal cortex perfusion has been shown to predict better neuropsychological response to cholinesterase inhibitors in elders with AD.[38] Thus, the current study reinforces the early vulnerability and predictive power of longitudinal volumetric study of non-hippocampal regions in healthy elders who possess an ε4 allele.

Widespread WM atrophy occurred in both carriers and non-carriers over the course of the five-year follow-up interval. GM atrophy appears to show a linear negative correlation with age, whereas age-related WM microstructure damage and atrophy appear to take place in a nonlinear fashion that does not correlate with, and may precede, GM atrophy.[39,40] Furthermore, WM atrophy in healthy elders has been associated with etiological factors that may be independent of AD-related neuropathology, e.g., hypertension[41,42] and depression.[43,44] Alternatively, it is conceivable that WM volumetric measures may be less sensitive to AD-related pathology than microstructural changes to WM as observed with diffusion tensor imaging.[45,46]

The current study identified specific hippocampal subfields, namely the CA2,3, CA4-DG, presubiculum and subiculum that appear to be vulnerable to atrophy in older carriers. Most of the previously published longitudinal studies (Table 1) were conducted at 1.5T.[7,8,10-14] The superior signal to noise ratio associated with 3T[47,48] is critical for delineating hippocampal subfields.[49]

Most prior studies examined longitudinal changes based on two examination periods. By scanning three times over the course of the five-year interval, we were in a position to determine if the atrophic

changes accelerate over time, as reflected by a significant quadratic effect. Our analyses, however, observed no evidence of a quadratic change, suggesting that the increases in atrophy were linear in nature.

The current study has its limitations. We were unable to assess AD-related pathology directly by examining CSF or PET markers of Aβ or tau pathology. It might also have been useful to examine inflammatory markers, such as Interleukin-6 (IL6), which can be associated with plaque formation.[50] Our analysis of hippocampal subfields used the automatic FreeSurfer parcellation method, which has been criticized by some for accuracy limitations.[51] Finally, future studies will require replication with a larger and more varied sex and ethnicity distribution.

The current study sheds light on the importance of longitudinal measurements of total and regional brain volumes for assessing AD-related neuropathology in genetically atrisk healthy elders. The success of future prevention studies hinges on the identification of biomarkers that are sensitive to AD-related neuropathology during the preclinical stage. Results of our study indicate that volumetric MRI may be a candidate biomarker in future prevention studies involving APOE ε4 carriers.

## Acknowledgements

## Conflict of interest

The authors declare no conflict of interest.

*Corresponding author: Schey Center for Cognitive Neuroimaging, Neurological Institute, Cleveland Clinic, 9500 Euclid Avenue/U10, Cleveland,

OH 44195, USA. Telephone: +1 216 444 1025; Fax: +1 216 445 7013; E-mail address: raos2@ccf.org (S.M. Rao).

# References

[1]Jack CR, Knopman DS, Jagust WJ, Shaw LM, Aisen PS, Weiner MW, Petersen RC, Trojanowski JQ (2010) Hypothetical model of dynamic biomarkers of the Alzheimer's pathological cascade. *The Lancet Neurology* **9**, 119-128.

[2]Bendlin BB, Carlsson CM, Gleason CE, Johnson SC, Sodhi A, Gallagher CL, Puglielli L, Engelman CD, Ries ML, Xu G, Wharton W, Asthana S (2010) Midlife predictors of Alzheimer's disease. *Maturitas* **65**, 131-137.

[3]Alzheimer's Association (2014) 2014 Alzheimer's disease facts and figures. *Alzheimer's & Dementia* **10**, e47-e92.

[4]Burggren AC, Zeineh M, Ekstrom AD, Braskie MN, Thompson PM, Small GW, Bookheimer SY (2008) Reduced cortical thickness in hippocampal subregions among cognitively normal apolipoprotein E e4 carriers. *Neuroimage* **41**, 1177-1183.

[5]Schuff N, Woerner N, Boreta L, Kornfield T, Shaw LM, Trojanowski JQ, Thompson PM, Jack CR, Jr., Weiner MW, Alzheimer's Disease Neuroimaging I (2009) MRI of hippocampal volume loss in early Alzheimer's disease in relation to ApoE genotype and biomarkers. *Brain* **132**, 1067-1077.

[6]Ball M, Hachinski V, Fox A, Kirshen A, Fisman M, Blume W, Kral V, Fox H, Merskey H (1985) A new definition of Alzheimer's disease: a hippocampal dementia. *The Lancet* **325**, 14-16.

[7]Jak AJ, Houston WS, Nagel BJ, Corey-Bloom J, Bondi MW (2007) Differential crosssectional and longitudinal impact of APOE genotype on hippocampal volumes in nondemented older adults. *Dement Geriatr Cogn Disord* **23**, 382-389.

[8]Moffat S, Szekely C, Zonderman A, Kabani N, Resnick S (2000) Longitudinal change in hippocampal volume as a function of apolipoprotein E genotype. *Neurology* **55**, 134-136.

[9]Rao SM, Bonner-Jackson A, Nielson KA, Seidenberg M, Smith JC, Woodard JL, Durgerian S (2015) Genetic risk for Alzheimer's disease alters the five-year trajectory of semantic memory activation in cognitively intact elders. *Neuroimage* **111**, 136-146.

[10]Lo RY, Hubbard AE, Shaw LM, Trojanowski JQ, Petersen RC, Aisen PS, Weiner MW, Jagust WJ, Alzheimer's Disease Neuroimaging I (2011) Longitudinal change of biomarkers in cognitive decline. *Arch Neurol* **68**, 1257-1266.

[11]Taylor JL, Scanlon BK, Farrell M, Hernandez B, Adamson MM, Ashford JW, Noda A, Murphy GM, Jr., Weiner MW (2014) APOE-epsilon4 and aging

of medial temporal lobe gray matter in healthy adults older than 50 years. *Neurobiol Aging* **35**, 2479-2485.

[12]Nosheny RL, Insel PS, Truran D, Schuff N, Jack CR, Jr., Aisen PS, Shaw LM, Trojanowski JQ, Weiner MW, Alzheimer's Disease Neuroimaging I (2015) Variables associated with hippocampal atrophy rate in normal aging and mild cognitive impairment. *Neurobiol Aging* **36**, 273-282.

[13]Crivello F, Lemaitre H, Dufouil C, Grassiot B, Delcroix N, Tzourio-Mazoyer N, Tzourio C, Mazoyer B (2010) Effects of ApoE-epsilon4 allele load and age on the rates of grey matter and hippocampal volumes loss in a longitudinal cohort of 1186 healthy elderly persons. *Neuroimage* **53**, 1064-1069.

[14]Lu PH, Thompson PM, Leow A, Lee GJ, Lee A, Yanovsky I, Parikshak N, Khoo T, Wu S, Geschwind D, Bartzokis G (2011) Apolipoprotein E genotype is associated with temporal and hippocampal atrophy rates in healthy elderly adults: a tensor-based morphometry study. *J Alzheimers Dis* **23**, 433-442.

[15]Raz N, Ghisletta P, Rodrigue KM, Kennedy KM, Lindenberger U (2010) Trajectories of brain aging in middle-aged and older adults: regional and individual differences. *Neuroimage* **51**, 501-511.

[16]Seidenberg M, Guidotti L, Nielson KA, Woodard JL, Durgerian S, Antuono P, Zhang Q, Rao SM (2009) Semantic memory activation in individuals at risk for developing Alzheimer disease. *Neurology* **73**, 612-620.

[17]Yesavage JA, Brink TL, Rose TL, Lum O, Huang V, Adey M, Leirer VO (1983) Development and validation of a geriatric depression screening scale: A preliminary report. *Journal of Psychiatric Research* **17**, 37.

[18]Lawton MP, Brody EM (1969) Assessment of Older People: Self-Maintaining and Instrumental Activities of Daily Living. *The Gerontologist* **9**, 179-186.

[19]O'Brien DP, Campbell KA, Morken NW, Bair RJ, Heath EM (2001) Automated Nucleic Acid Purification for Large Samples. *Journal of the Association for Laboratory Automation* **6**, 67-70.

[20]Folstein MF, Folstein SE, McHugh PR (1975) "Mini-mental state": A practical method for grading the cognitive state of patients for the clinician. *Journal of Psychiatric Research* **12**, 189-198.

[21]Jurica PJ, Leitten CL, Mattis S (2001) *DRS-2 dementia rating scale-2: Professional manual*, Psychological Assessment Resources, Lutz, FL.

[22]Rey A (1958) L'examen clinique en psychologie.

[23]Reuter M, Schmansky NJ, Rosas HD, Fischl B (2012) Within-subject template estimation for unbiased longitudinal image analysis. *Neuroimage* **61**, 1402-1418.

[24]Adalbert R, Gilley J, Coleman MP (2007) Abeta, tau and ApoE4 in Alzheimer's disease: the axonal connection. *Trends Mol Med* **13**, 135-142.

[25]Huang Y, Mucke L (2012) Alzheimer mechanisms and therapeutic strategies. *Cell* **148**, 1204-1222.

[26]Morris JC, Roe CM, Xiong C, Fagan AM, Goate AM, Holtzman DM, Mintun MA (2010) APOE predicts amyloid-beta but not tau Alzheimer pathology in cognitively normal aging. *Ann Neurol* **67**, 122-131.

[27]Liu CC, Kanekiyo T, Xu H, Bu G (2013) Apolipoprotein E and Alzheimer disease: risk, mechanisms and therapy. *Nat Rev Neurol* **9**, 106-118.

[28]Mormino EC, Kluth JT, Madison CM, Rabinovici GD, Baker SL, Miller BL, Koeppe RA, Mathis CA, Weiner MW, Jagust WJ, Alzheimer's Disease Neuroimaging I (2008) Episodic memory loss is related to hippocampal-mediated beta-amyloid deposition in elderly subjects. *Brain* **132**, 1310-1323.

[29]Du A, Schuff N, Amend D, Laakso M, Hsu Y, Jagust W, Yaffe K, Kramer J, Reed B, Norman D (2001) Magnetic resonance imaging of the entorhinal cortex and hippocampus in mild cognitive impairment and Alzheimer's disease. *Journal of Neurology, Neurosurgery & Psychiatry* **71**, 441-447.

[30]Mueller SG, Schuff N, Raptentsetsang S, Elman J, Weiner MW (2008) Selective effect of Apo e4 on CA3 and dentate in normal aging and Alzheimer's disease using high resolution MRI at 4 T. *Neuroimage* **42**, 42-48.

[31]Apostolova LG, Mosconi L, Thompson PM, Green AE, Hwang KS, Ramirez A, Mistur R, Tsui WH, de Leon MJ (2010) Subregional hippocampal atrophy predicts Alzheimer's dementia in the cognitively normal. *Neurobiol Aging* **31**, 1077-1088.

[32]Chou YY, Lepore N, de Zubicaray GI, Carmichael OT, Becker JT, Toga AW, Thompson PM (2008) Automated ventricular mapping with multi-atlas fluid image alignment reveals genetic effects in Alzheimer's disease. *Neuroimage* **40**, 615-630.

[33]Nestor SM, Rupsingh R, Borrie M, Smith M, Accomazzi V, Wells JL, Fogarty J, Bartha R, Alzheimer's Disease Neuroimaging I (2008) Ventricular enlargement as a possible measure of Alzheimer's disease progression validated using the Alzheimer's disease neuroimaging initiative database. *Brain* **131**, 2443-2454.

[34]Tosun D, Schuff N, Truran-Sacrey D, Shaw LM, Trojanowski JQ, Aisen P, Peterson R, Weiner MW, Alzheimer's Disease Neuroimaging I (2010) Relations between brain tissue loss, CSF biomarkers, and the ApoE genetic profile: a longitudinal MRI study. *Neurobiol Aging* **31**, 1340-1354.

[35]Reiman EM, Caselli RJ, Chen K, Alexander GE, Bandy D, Frost J (2001) Declining brain activity in cognitively normal apolipoprotein E epsilon 4 heterozygotes: A foundation for using positron emission tomography

to efficiently test treatments to prevent Alzheimer's disease. *Proc Natl Acad Sci U S A* **98**, 3334-3339.

[36]Chetelat G, Landeau B, Eustache F, Mezenge F, Viader F, de la Sayette V, Desgranges B, Baron JC (2005) Using voxel-based morphometry to map the structural changes associated with rapid conversion in MCI: a longitudinal MRI study. *Neuroimage* **27**, 934-946.

[37]McEvoy LK, Fennema-Notestine C, Roddey JC, Hagler DJ, Jr., Holland D, Karow DS, Pung CJ, Brewer JB, Dale AM, Alzheimer's Disease Neuroimaging I (2009) Alzheimer disease: quantitative structural neuroimaging for detection and prediction of clinical and structural changes in mild cognitive impairment. *Radiology* **251**, 195-205.

[38]Mega MS, Dinov ID, Lee L, O'Connor SM, Masterman DM, Wilen B, Mishkin F, Toga AW, Cummings JL (2000) Orbital and Dorsolateral Frontal Perfusion Defect Associated With Behavioral Response to Cholinesterase Inhibitor Therapy in Alzheimer's Disease. *The Journal of Neuropsychiatry and Clinical Neurosciences* **12**, 209-218.

[39]Agosta F, Pievani M, Sala S, Geroldi C, Galluzzi S, Frisoni GB, Filippi M (2011) White Matter Damage in Alzheimer Disease and Its Relationship to Gray Matter Atrophy. *Radiology* **258**, 853-863.

[40]Giorgio A, Santelli L, Tomassini V, Bosnell R, Smith S, De Stefano N, Johansen-Berg H (2010) Age-related changes in grey and white matter structure throughout adulthood. *Neuroimage* **51**, 943-951.

[41]de Leeuw FE, Richard F, de Groot JC, van Duijn CM, Hofman A, Van Gijn J, Breteler MM (2004) Interaction between hypertension, apoE, and cerebral white matter lesions. *Stroke* **35**, 1057-1060.

[42]van Dijk EJ, Breteler MM, Schmidt R, Berger K, Nilsson LG, Oudkerk M, Pajak A, Sans S, de Ridder M, Dufouil C, Fuhrer R, Giampaoli S, Launer LJ, Hofman A, Consortium C (2004) The association between blood pressure, hypertension, and cerebral white matter lesions: cardiovascular determinants of dementia study. *Hypertension* **44**, 625-630.

[43]de Groot JC, de Leeuw FE, Oudkerk M, Hofman A, Jolles J, Breteler MMB (2000) Cerebral White Matter Lesions and Depressive Symptoms in Elderly Adults. *Archives of General Psychiatry* **57**, 1071-1076.

[44]Janssen J, Hulshoff Pol HE, de Leeuw FE, Schnack HG, Lampe IK, Kok RM, Kahn RS, Heeren TJ (2007) Hippocampal volume and subcortical white matter lesions in late life depression: comparison of early and late onset depression. *J Neurol Neurosurg Psychiatry* **78**, 638-640.

[45]Persson J, Lind J, Larsson A, Ingvar M, Cruts M, Van Broeckhoven C, Adolfsson R, Nilsson LG, Nyberg L (2006) Altered brain white matter integrity in healthy carriers of the APOE ε4 allele: A risk for AD? *Neurology* **66**, 1029-1033.

[46]Ryan L, Walther K, Bendlin BB, Lue LF, Walker DG, Glisky EL (2011) Age-related differences in white matter integrity and cognitive function are related to APOE status. *Neuroimage* **54**, 1565-1577.

[47]Alvarez-Linera J (2008) 3T MRI: advances in brain imaging. *Eur J Radiol* **67**, 415-426.

[48]Willinek WA, Schild HH (2008) Clinical advantages of 3.0 T MRI over 1.5 T. *Eur J Radiol* **65**, 2-14.

[49]Chow N, Hwang KS, Hurtz S, Green AE, Somme JH, Thompson PM, Elashoff DA, Jack CR, Weiner M, Apostolova LG, Alzheimer's Disease Neuroimaging I (2015) Comparing 3T and 1.5T MRI for mapping hippocampal atrophy in the Alzheimer's Disease Neuroimaging Initiative. *AJNR Am J Neuroradiol* **36**, 653-660.

[50]Licastro F, Pedrini S, Caputo L, Giorgio A, Davis LJ, Ferri C, Casadei V, Grimaldi LME (2000) Increased plasma levels of interleukin-1, interleukin-6 and α-1- antichymotrypsin in patients with Alzheimer's disease: peripheral inflammation or signals from the brain? *Journal of Neuroimmunology* **103**, 97-102.

[51]Wisse LE, Biessels GJ, Geerlings MI (2014) A Critical Appraisal of the Hippocampal Subfield Segmentation Package in FreeSurfer. *Front Aging Neurosci* **6**, 261.

## Figure Legend:

**Figure 1.** Longitudinal volumetric change in the left and right total hippocampi (top), right CA2,3 and CA4,DG hippocampal subfields (middle), and left and right lateral ventricles (bottom) for the APOE e4+ (blue) and e4- (green) groups. The x axis plots time in study, indexed in years; y axis indicates brain volume as a percent of intracranial volume. Error bars = s.e.m.
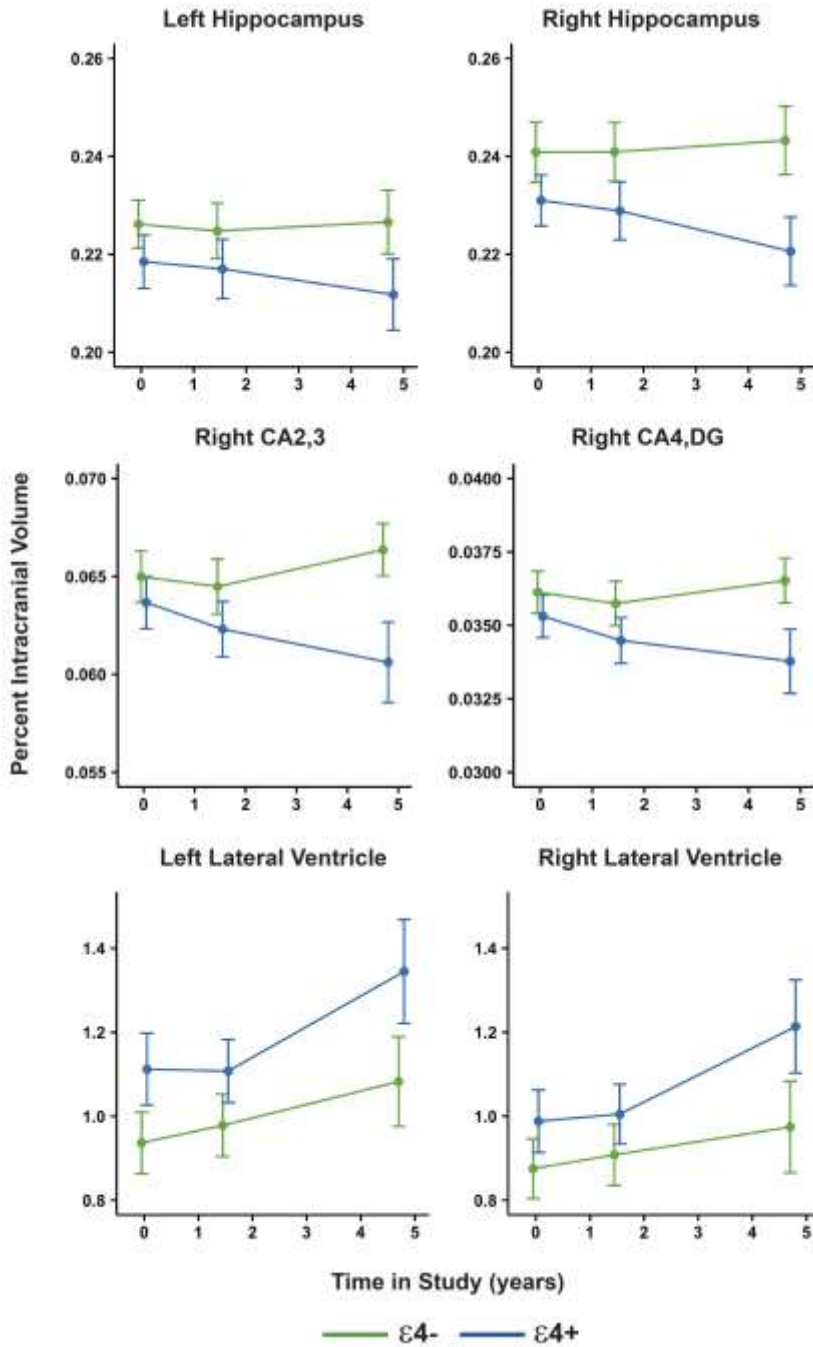
**Table 1:** Longitudinal changes in hippocampal and non-hippocampal volume in APOE ε4+ and ε4- elders who were cognitively intact and healthy at study entry.

| Study | Sample Source | ε4+ | | ε4- | | Scan Interval (mos) | Number of time points | Analysis Method | Baseline HC Volume | Δ in HC Volume | Δ in non-HC Volume |
|---|---|---|---|---|---|---|---|---|---|---|---|
| | | N | Age M (SD) | N | Age M (SD) | | | | | | |
| Moffat 2000 | BLSA | 13 | 68.5 (5.9) | 13 | 69.7 (6.8) | 31 | 2 | MT | ε4+ = ε4- | ε4+ > ε4- | WBV: ε4+ = ε4- |
| Jak 2007 | Local | 8 | 74.9 (7.2) | 26 | 77.6 (6.7) | 17 | 2 | AFNI, MT | ε4+ = ε4- | ε4+ > ε4- | NR |
| Crivello 2010 | 3C | 239 ε3/ε4 14 ε4/ε4 | ε3/ε4: 72.0 (3.9) ε4/ε4: 71.0 (2.3) | 933 | 72.4 (4.0) | 48 | 2 | VBM | NR | ε4/ε4 > ε4/ε3; ε4/ε4 > ε4- | Total GM: ε4/ε4 > ε4/ε3; ε4/ε4 > ε4- |
| Lo 2011 | ADNI | 61 | NR | 168 | NR | 36 | 2-6 | FreeSurfer | ε4+ = ε4- | ε4+ = ε4- | NR |
| Lu 2011 | Local | 16 | 65 (4.5) | 11 | 67.0 (5.2) | 56 | 2 | BrainSuite | NR | ε4+ > ε4-*; RH>LH | TC: ε4+ > ε4-* |
| Taylor 2014 | Aviation | 25 | 59.4 (5.7) | 31 | 62.2 (6.3) | 38 | 2 | SNT | ε4+ < ε4- | ε4+ = ε4- | MTL: ε4+ = ε4- |
| Nosheny 2015 | ADNI | 55 | NR | 153 | NR | 48 | 2-6 | FreeSurfer | NR | ε4+ = ε4- | NR |
| Rao 2015 | Local | 24 | 72.5 (4.1) | 21 | 73.2 (5.3) | 57 | 3 | FreeSurfer | ε4+ = ε4- | ε4+ > ε4-^ | NR |

Notes: MRI was reported at 1.5T in all studies except Moffat et al. (2000), which was unspecified and Rao et al. (2015) reported 3T; ^ = bilateral measurement; 3C=Three City Study (France); AD=Alzheimer's disease; ADNI=Alzheimer's Disease Neuroimaging Initiative; Aviation=Stanford/VA Aviation Study; BLSA=Baltimore Longitudinal Study of Aging; ε4+=presence of an ε4 allele; ε4-=ε4 non-carrier; ε4-*=non-ε4 carrier with presence of an ε2 allele; GM=grey matter; HC=hippocampus; MT= Manual tracing; MTL=medial temporal lobes; NR= not reported for this group or comparison; TC=temporal cortex.

**Table 2:** Baseline characteristics of ε4+ and ε4- groups

| Variable | ε4-<br>(N=30) | ε4+<br>(N=42) | p* | partial $\eta^2$ |
|---|---|---|---|---|
| Age (mean yrs, SD) | 73.94 (5.38) | 73.02 (4.98) | 0.45 | 0.01 |
| Sex (N, % Female) | 23, 77% | 28, 67% | 0.44 | 0.01 |
| Education (mean yrs, SD) | 14.33 (2.32) | 15.57 (2.91) | 0.06 | 0.05 |
| Family History (N, % Yes) | 0, 0% | 28, 67% | -- | -- |
| ADL | 5.00 (0.00) | 5.00 (0.00) | -- | -- |
| GDS | 1.90 (2.29) | 2.38 (2.72) | 0.43 | 0.01 |
| MMSE | 29.33 (0.80) | 28.83 (1.30) | 0.07 | 0.05 |
| DRS Total | 140.40 (3.21) | 139.38 (4.08) | 0.26 | 0.02 |
|   Attention | 36.53 (0.68) | 36.36 (0.85) | 0.35 | 0.01 |
|   Initiation/Perseveration | 36.63 (0.80) | 36.36 (1.81) | 0.44 | 0.01 |
|   Construction | 6.00 (0.00) | 5.98 (0.15) | 0.40 | 0.01 |
|   Concentration | 37.03 (3.12) | 37.17 (1.83) | 0.82 | 0.00 |
|   Memory | 24.20 (1.00) | 23.71 (1.88) | 0.20 | 0.02 |
| RAVLT | | | | |
|   Learning | 48.77 (7.70) | 46.10 (8.97) | 0.19 | 0.02 |
|   Immediate Recall | 9.63 (2.13) | 8.81 (2.70) | 0.17 | 0.03 |
|   Delayed Recall | 9.97 (1.94) | 8.93 (3.01) | 0.10 | 0.04 |

Notes: ε4+ = ε4 allele carrier; ε4- = ε4 allele non-carrier; ADL = Activities of Daily Living; GDS = Geriatric Depression Scale; MMSE = Mini Mental State Examination; DRS = Dementia Rating Scale; RAVLT = Rey Auditory Verbal Learning Test
*p-values derived from Student's t-test, except for sex (Fisher's exact test)

**Table 3:** Coefficients (±SEM) from linear mixed effects of total hippocampal volumes and parcellated hippocampal subfields

| Region | Intercept (baseline) | | Slope (time) | |
|---|---|---|---|---|
| | ε4-[a] | ε4+ vs ε4-[b] | ε4-[c] | ε4+ vs ε4-[d] |
| Left Hemisphere | | | | |
| Total Hippocampus | 3.174 (0.063) | -0.102 (0.083) | -0.011 (0.008) | **-0.026 (0.010)** |
| CA1 | 0.303 (0.005) | -0.003 (0.007) | 0.001 (0.001) | 0.000 (0.001) |
| CA2.3 | 0.854 (0.019) | -0.034 (0.025) | -0.005 (0.002) | -0.002 (0.003) |
| CA4.DG | 0.482 (0.010) | -0.019 (0.013) | -0.003 (0.001) | -0.001 (0.001) |
| Fimbria | 0.040 (0.003) | 0.007 (0.004) | 0.000 (0.001) | 0.000 (0.001) |
| Hippocampal Fissure | 0.051 (0.004) | 0.003 (0.005) | 0.000 (0.001) | 0.000 (0.001) |
| Presubiculum | 0.392 (0.009) | -0.019 (0.012) | -0.003 (0.002) | -0.003 (0.002) |
| Subiculum | 0.556 (0.01) | -0.024 (0.013) | -0.003 (0.001) | -0.001 (0.002) |
| Right Hemisphere | | | | |
| Total Hippocampus | 3.397 (0.064) | -0.154 (0.084) | -0.010 (0.009) | **-0.032 (0.012)** |
| CA1 | 0.310 (0.007) | -0.007 (0.009) | 0.000 (0.001) | -0.001 (0.001) |
| CA2.3 | 0.913 (0.019) | -0.017 (0.025) | -0.002 (0.002) | **-0.007 (0.002)** |
| CA4.DG | 0.509 (0.010) | -0.014 (0.013) | -0.002 (0.001) | **-0.004 (0.001)** |
| Fimbria | 0.045 (0.003) | 0.001 (0.004) | -0.001 (0.001) | 0.000 (0.001) |
| Hippocampal Fissure | 0.052 (0.004) | 0.011 (0.005) | 0.000 (0.001) | 0.000 (0.001) |
| Presubiculum | 0.381 (0.008) | -0.015 (0.010) | -0.001 (0.001) | **-0.004 (0.002)** |
| Subiculum | 0.555 (0.009) | -0.025 (0.013) | -0.001 (0.001) | **-0.005 (0.002)** |

Notes: All values in mL; ε4+ = ε4 allele carrier; ε4- = ε4 allele non-carrier; CA = cornu ammonis; DG = dentate gyrus; **Bolded** values are statistically significant after controlling for multiple comparisons using false discovery rate

[a] Predicted mean intercept (baseline) of each region. Standard errors of coefficients are in parentheses.

[b] Predicted mean intercept (baseline) of each structure by presence of ε4. Standard errors of coefficients are in parentheses.

[c] Predicted average yearly rate of change (slope). Standard errors of coefficients are in parentheses.

[d] Predicted average yearly rate of change (slope) by presence of ε4. Standard errors of coefficients are in parentheses.

**Table 4:** Coefficients (±SEM) from linear mixed effects of global cortical grey and white matter and ventricular volumes

| Region | Intercept (baseline) | | Slope (time) | |
|---|---|---|---|---|
| | ε4-[a] | ε4+ vs ε4-[b] | ε4-[c] | ε4+ vs ε4-[d] |
| **Left Hemisphere** | | | | |
| Cortical GM Volume | 207.534 (2.296) | -0.147 (3.041) | 0.060 (0.285) | **-0.877 (0.378)** |
| Cortical WM Volume | 219.268 (3.552) | -4.747 (4.701) | **-1.532 (0.242)** | -0.129 (0.32) |
| Lateral Ventricle | 13.911 (1.193) | 1.914 (1.578) | **0.447 (0.069)** | **0.305 (0.09)** |
| Inferior Lateral Ventricle | 0.782 (0.075) | 0.023 (0.1) | **0.025 (0.011)** | **0.032 (0.014)** |
| **Right Hemisphere** | | | | |
| Cortical GM Volume | 207.864 (2.381) | 0.881 (3.152) | -0.019 (0.26) | **-0.762 (0.345)** |
| Cortical WM Volume | 219.548 (3.601) | -5.141 (4.769) | **-1.490 (0.204)** | -0.197 (0.27) |
| Lateral Ventricle | 13.058 (1.012) | 1.001 (1.337) | **0.438 (0.069)** | **0.296 (0.091)** |
| Inferior Lateral Ventricle | 0.631 (0.05) | 0.009 (0.066) | **0.016 (0.01)** | **0.039 (0.013)** |
| Third Ventricle | 1.554 (0.087) | 0.046 (0.115) | **0.034 (0.005)** | **0.015 (0.007)** |
| Fourth Ventricle | 1.994 (0.095) | 0.180 (0.126) | **0.021 (0.012)** | -0.013 (0.015) |

Notes: all values in mL; ε4+ = ε4 allele carrier; ε4- = ε4 allele non-carrier; GM=gray matter; WM=white matter; **Bolded** values are statistically significant after controlling for multiple comparisons using false discovery rate

[a] Predicted mean intercept (baseline) of each region. Standard errors of coefficients are in parentheses.

[b] Predicted mean intercept (baseline) of each structure by presence of ε4. Standard errors of coefficients are in parentheses.

[c] Predicted average yearly rate of change (slope). Standard errors of coefficients are in parentheses.

[d] Predicted average yearly rate of change (slope) by presence of ε4. Standard errors of coefficients are in parentheses.

**Table 5:** Coefficients (±SEM) from linear mixed effects of Right Hemisphere parcellated cortical grey matter regions

| Right Hemisphere Region | Intercept (baseline) | | Slope (time) | |
|---|---|---|---|---|
| | ε4-[a] | ε4+ vs ε4-[b] | ε4-[c] | ε4+ vs ε4-[d] |
| Bankssts | 2.057 (0.051) | -0.002 (0.067) | -0.008 (0.004) | -0.003 (0.006) |
| Caudal anterior cingulate | 2.145 (0.083) | -0.104 (0.11) | -0.004 (0.004) | -0.002 (0.006) |
| Caudal middle frontal | 5.683 (0.173) | -0.101 (0.23) | 0.015 (0.011) | -0.019 (0.015) |
| Cuneus | 2.933 (0.08) | 0.000 (0.105) | -0.003 (0.006) | 0.007 (0.008) |
| Entorhinal | 1.715 (0.069) | -0.065 (0.091) | -0.010 (0.009) | -0.004 (0.013) |
| Frontal pole | 1.000 (0.032) | 0.053 (0.042) | -0.001 (0.003) | -0.005 (0.004) |
| Fusiform | 7.990 (0.138) | 0.319 (0.182) | 0.022 (0.017) | -0.054 (0.022) |
| Inferior parietal | 14.325 (0.285) | -0.127 (0.377) | -0.066 (0.026) | -0.033 (0.035) |
| Inferior temporal | 8.941 (0.185) | 0.111 (0.245) | -0.018 (0.023) | -0.052 (0.031) |
| Insula | 6.546 (0.136) | 0.259 (0.181) | -0.005 (0.012) | 0.002 (0.016) |
| Isthmus cingulate | 2.328 (0.062) | -0.015 (0.082) | 0.001 (0.004) | -0.008 (0.005) |
| Lateral occipital | 10.076 (0.215) | 0.684 (0.285) | -0.022 (0.033) | -0.015 (0.044) |
| Lateral OFC | 6.846 (0.129) | -0.060 (0.171) | 0.032 (0.011) | **-0.046 (0.015)** |
| Lingual | 5.866 (0.136) | 0.010 (0.18) | 0.030 (0.012) | **-0.043 (0.015)** |
| Medial OFC | 4.776 (0.085) | 0.013 (0.113) | -0.001 (0.011) | -0.026 (0.014) |
| Middle temporal | 10.342 (0.225) | -0.050 (0.298) | -0.035 (0.024) | -0.068 (0.031) |
| Paracentral | 3.726 (0.096) | -0.021 (0.127) | -0.002 (0.009) | -0.024 (0.012) |
| Parahippocampal | 1.821 (0.044) | 0.035 (0.058) | -0.004 (0.004) | **-0.015 (0.005)** |
| Pars opercularis | 3.526 (0.102) | 0.091 (0.136) | -0.001 (0.006) | -0.011 (0.008) |
| Pars orbitalis | 2.362 (0.068) | 0.131 (0.091) | -0.005 (0.005) | -0.001 (0.007) |
| Pars triangularis | 3.630 (0.105) | 0.037 (0.139) | -0.010 (0.006) | 0.007 (0.008) |
| Pericalcarine | 2.270 (0.069) | -0.021 (0.091) | -0.004 (0.005) | -0.007 (0.007) |
| Postcentral | 8.521 (0.189) | -0.058 (0.25) | -0.003 (0.012) | 0.002 (0.016) |
| Posterior cingulate | 3.132 (0.083) | -0.119 (0.11) | -0.008 (0.005) | -0.012 (0.007) |
| Precentral | 12.373 (0.241) | 0.224 (0.319) | -0.008 (0.022) | -0.029 (0.029) |
| Precuneus | 9.095 (0.159) | -0.216 (0.211) | 0.002 (0.015) | -0.035 (0.02) |
| Rostral anterior cingulate | 1.951 (0.062) | 0.065 (0.082) | 0.003 (0.005) | -0.009 (0.007) |
| Rostral middle frontal | 14.362 (0.277) | -0.211 (0.367) | 0.015 (0.029) | -0.055 (0.039) |
| Superior frontal | 18.589 (0.269) | 0.443 (0.356) | 0.003 (0.043) | -0.065 (0.057) |
| Superior parietal | 12.890 (0.268) | -0.484 (0.354) | -0.006 (0.027) | -0.029 (0.036) |
| Supramarginal | 9.538 (0.207) | -0.220 (0.274) | -0.022 (0.014) | -0.022 (0.018) |
| Superior temporal | 9.678 (0.202) | 0.334 (0.267) | -0.016 (0.017) | -0.053 (0.023) |
| Temporal pole | 2.201 (0.076) | 0.179 (0.101) | 0.001 (0.01) | -0.005 (0.013) |
| Transverse temporal | 0.843 (0.029) | 0.003 (0.039) | **-0.007 (0.002)** | 0.002 (0.002) |

Notes: All values in mL; bankssts=banks of the superior temporal sulcus; ε4+ = ε4 allele carrier; ε4- = ε4 allele non-carrier; OFC=orbitofrontal cortex; **Bolded** values are statistically significant after controlling for multiple comparisons using false discovery rate

[a] Predicted mean intercept (baseline) of each region. Standard errors of coefficients are in parentheses.

[b] Predicted mean intercept (baseline) of each structure by presence of ε4. Standard errors of coefficients are in parentheses.

[c] Predicted average yearly rate of change (slope). Standard errors of coefficients are in parentheses.

[d] Predicted average yearly rate of change (slope) by presence of ε4. Standard errors of coefficients are in parentheses.

**Table 6:** Coefficients (±SEM) from linear mixed effects of Left Hemisphere parcellated cortical grey matter regions

| Left Hemisphere Region | Intercept (baseline) | | Slope (time) | |
|---|---|---|---|---|
| | ε4-[a] | ε4+ vs ε4-[b] | ε4-[c] | ε4+ vs ε4-[d] |
| Bankssts | 2.201 (0.075) | 0.029 (0.099) | -0.005 (0.005) | -0.006 (0.007) |
| Caudal anterior cingulate | 1.809 (0.065) | -0.051 (0.086) | -0.001 (0.004) | -0.006 (0.006) |
| Caudal middle frontal | 5.784 (0.149) | 0.310 (0.197) | 0.027 (0.014) | -0.031 (0.019) |
| Cuneus | 2.775 (0.06) | 0.019 (0.08) | 0.007 (0.006) | -0.011 (0.008) |
| Entorhinal | 1.642 (0.055) | 0.099 (0.073) | 0.004 (0.01) | -0.027 (0.014) |
| Frontal pole | 0.796 (0.033) | 0.018 (0.044) | -0.004 (0.003) | -0.001 (0.004) |
| Fusiform | 8.212 (0.19) | 0.126 (0.252) | 0.048 (0.023) | -0.062 (0.03) |
| Inferior parietal | 12.831 (0.281) | -0.695 (0.373) | -0.060 (0.026) | -0.034 (0.034) |
| Inferior temporal | 9.250 (0.224) | 0.240 (0.297) | -0.018 (0.021) | -0.060 (0.028) |
| Insula | 6.558 (0.117) | -0.007 (0.155) | 0.005 (0.009) | -0.024 (0.012) |
| Isthmus cingulate | 2.533 (0.072) | -0.021 (0.095) | 0.006 (0.004) | -0.007 (0.005) |
| Lateral occipital | 10.469 (0.214) | 0.431 (0.283) | -0.009 (0.038) | -0.007 (0.051) |
| Lateral OFC | 6.904 (0.106) | 0.098 (0.14) | 0.000 (0.012) | -0.030 (0.015) |
| Lingual | 5.716 (0.144) | 0.078 (0.19) | **0.046 (0.013)** | **-0.055 (0.017)** |
| Medial OFC | 5.100 (0.106) | 0.038 (0.141) | -0.016 (0.018) | -0.016 (0.018) |
| Middle temporal | 9.537 (0.208) | -0.467 (0.275) | **-0.089 (0.02)** | -0.013 (0.027) |
| Paracentral | 3.343 (0.088) | 0.017 (0.117) | 0.000 (0.007) | -0.013 (0.009) |
| Parahippocampal | 1.876 (0.049) | 0.126 (0.064) | 0.009 (0.006) | **-0.023 (0.008)** |
| Pars opercularis | 4.320 (0.113) | 0.040 (0.149) | -0.003 (0.007) | -0.011 (0.009) |
| Pars orbitalis | 1.954 (0.048) | 0.018 (0.063) | **-0.015 (0.004)** | -0.012 (0.006) |
| Pars triangularis | 3.075 (0.085) | 0.040 (0.113) | -0.012 (0.005) | 0.000 (0.007) |
| Pericalcarine | 2.044 (0.061) | -0.081 (0.081) | 0.004 (0.005) | -0.007 (0.007) |
| Postcentral | 8.978 (0.186) | 0.163 (0.246) | 0.018 (0.015) | -0.032 (0.019) |
| Posterior cingulate | 3.055 (0.083) | -0.144 (0.11) | -0.002 (0.006) | -0.015 (0.007) |
| Precentral | 12.460 (0.206) | -0.167 (0.273) | -0.005 (0.024) | -0.042 (0.032) |
| Precuneus | 8.801 (0.145) | -0.136 (0.193) | 0.017 (0.017) | -0.048 (0.023) |
| Rostral anterior cingulate | 2.365 (0.075) | 0.121 (0.099) | 0.014 (0.006) | -0.015 (0.007) |
| Rostral middle frontal | 13.570 (0.27) | 0.065 (0.357) | 0.034 (0.026) | -0.063 (0.034) |
| Superior frontal | 19.910 (0.332) | -0.248 (0.439) | 0.022 (0.04) | -0.060 (0.053) |
| Superior parietal | 12.564 (0.261) | -0.222 (0.346) | 0.001 (0.027) | -0.039 (0.036) |
| Supramarginal | 9.897 (0.212) | -0.231 (0.281) | -0.013 (0.018) | -0.051 (0.023) |
| Superior temporal | 9.941 (0.185) | 0.198 (0.245) | **-0.077 (0.019)** | -0.008 (0.026) |
| Temporal pole | 2.413 (0.055) | 0.064 (0.073) | -0.012 (0.013) | 0.009 (0.017) |
| Transverse temporal | 1.105 (0.038) | -0.045 (0.051) | -0.007 (0.003) | -0.002 (0.004) |

Notes: All values in mL; bankssts=banks of the superior temporal sulcus; ε4+ = ε4 allele carrier; ε4- = ε4 allele non-carrier; OFC=orbitofrontal cortex; **Bolded** values are statistically significant after controlling for multiple comparisons using false discovery rate

[a] Predicted mean intercept (baseline) of each region. Standard errors of coefficients are in parentheses.

[b] Predicted mean intercept (baseline) of each structure by presence of ε4. Standard errors of coefficients are in parentheses.

[c] Predicted average yearly rate of change (slope). Standard errors of coefficients are in parentheses.

[d] Predicted average yearly rate of change (slope) by presence of ε4. Standard errors of coefficients are in parentheses.

**Table 7:** Coefficients (±SEM) from linear mixed effects of Right Hemisphere parcellated cortical white matter regions

| Right Hemisphere Region | Intercept (baseline) | | Slope (time) | |
|---|---|---|---|---|
| | ε4-[a] | ε4+ vs ε4-[b] | ε4-[c] | ε4+ vs ε4-[d] |
| Bankssts | 2.615 (0.075) | -0.120 (0.1) | **-0.016 (0.003)** | -0.001 (0.004) |
| Caudal anterior cingulate | 2.827 (0.065) | -0.194 (0.086) | **-0.030 (0.006)** | -0.008 (0.007) |
| Caudal middle frontal | 5.480 (0.119) | 0.020 (0.158) | 0.005 (0.007) | -0.018 (0.01) |
| Cuneus | 2.045 (0.06) | -0.022 (0.079) | 0.007 (0.009) | 0.009 (0.012) |
| Entorhinal | 0.640 (0.027) | -0.023 (0.036) | **-0.006 (0.004)** | -0.004 (0.005) |
| Frontal pole | 0.331 (0.013) | 0.007 (0.018) | **-0.007 (0.002)** | -0.002 (0.003) |
| Fusiform | 5.856 (0.127) | 0.030 (0.168) | **-0.032 (0.009)** | -0.028 (0.012) |
| Inferior parietal | 10.890 (0.214) | -0.485 (0.283) | **-0.081 (0.013)** | 0.003 (0.017) |
| Inferior temporal | 5.176 (0.138) | -0.159 (0.183) | **-0.055 (0.011)** | -0.014 (0.015) |
| Insula | 8.320 (0.172) | 0.275 (0.228) | -0.013 (0.009) | -0.010 (0.013) |
| Isthmus cingulate | 3.270 (0.079) | -0.066 (0.104) | **-0.009 (0.005)** | -0.006 (0.007) |
| Lateral occipital | 7.789 (0.182) | 0.112 (0.241) | **-0.057 (0.022)** | 0.017 (0.029) |
| Lateral OFC | 6.506 (0.137) | -0.339 (0.182) | **-0.020 (0.008)** | -0.011 (0.01) |
| Lingual | 4.850 (0.122) | -0.053 (0.161) | 0.010 (0.012) | -0.003 (0.017) |
| Medial OFC | 3.251 (0.063) | 0.032 (0.084) | **-0.022 (0.008)** | -0.009 (0.011) |
| Middle temporal | 5.391 (0.124) | -0.209 (0.164) | **-0.076 (0.013)** | 0.005 (0.017) |
| Paracentral | 4.426 (0.117) | -0.117 (0.155) | -0.006 (0.009) | 0.019 (0.012) |
| Parahippocampal | 1.526 (0.041) | -0.026 (0.054) | **-0.015 (0.004)** | -0.003 (0.006) |
| Pars opercularis | 3.020 (0.095) | 0.036 (0.125) | **-0.013 (0.004)** | -0.014 (0.005) |
| Pars orbitalis | 1.117 (0.036) | 0.009 (0.048) | **-0.015 (0.004)** | -0.002 (0.005) |
| Pars triangularis | 2.998 (0.081) | -0.078 (0.107) | **-0.020 (0.006)** | -0.008 (0.008) |
| Pericalcarine | 2.873 (0.094) | 0.037 (0.125) | 0.005 (0.007) | 0.015 (0.009) |
| Postcentral | 6.907 (0.147) | -0.156 (0.195) | -0.003 (0.013) | -0.005 (0.017) |
| Posterior cingulate | 4.109 (0.08) | -0.193 (0.106) | **-0.040 (0.006)** | -0.009 (0.008) |
| Precentral | 13.199 (0.275) | -0.011 (0.364) | -0.020 (0.019) | 0.005 (0.025) |
| Precuneus | 9.166 (0.207) | -0.275 (0.275) | **-0.022 (0.012)** | 0.005 (0.016) |
| Rostral anterior cingulate | 2.003 (0.052) | -0.026 (0.068) | **-0.013 (0.004)** | -0.005 (0.005) |
| Rostral middle frontal | 11.655 (0.248) | -0.751 (0.329) | **-0.093 (0.019)** | -0.004 (0.025) |
| Superior frontal | 15.989 (0.31) | -0.065 (0.41) | **-0.076 (0.029)** | -0.019 (0.038) |
| Superior parietal | 11.124 (0.231) | -0.675 (0.306) | **-0.040 (0.017)** | 0.008 (0.023) |
| Supramarginal | 8.495 (0.182) | -0.396 (0.241) | **-0.040 (0.009)** | -0.006 (0.012) |
| Superior temporal | 6.213 (0.132) | 0.095 (0.174) | **-0.058 (0.012)** | -0.003 (0.016) |
| Temporal pole | 0.621 (0.021) | 0.018 (0.028) | **-0.008 (0.005)** | -0.005 (0.006) |
| Transverse temporal | 0.627 (0.021) | -0.033 (0.028) | -0.003 (0.002) | -0.002 (0.003) |

Notes: All values in mL; bankssts=banks of the superior temporal sulcus; ε4+ = ε4 allele carrier; ε4- = ε4 allele non-carrier; OFC=orbitofrontal cortex; **Bolded** values are statistically significant after controlling for multiple comparisons using false discovery rate

[a] Predicted mean intercept (baseline) of each region. Standard errors of coefficients are in parentheses.

[b] Predicted mean intercept (baseline) of each structure by presence of ε4. Standard errors of coefficients are in parentheses.

[c] Predicted average yearly rate of change (slope). Standard errors of coefficients are in parentheses.

[d] Predicted average yearly rate of change (slope) by presence of ε4. Standard errors of coefficients are in parentheses.

**Table 8:** Coefficients (±SEM) from linear mixed effects of Left Hemisphere parcellated cortical white matter regions

| Left Hemisphere Region | Intercept (baseline) | | Slope (time) | |
|---|---|---|---|---|
| | ε4-[a] | ε4+ vs ε4-[b] | ε4-[c] | ε4+ vs ε4-[d] |
| Bankssts | 2.775 (0.093) | -0.124 (0.123) | **-0.015 (0.003)** | -0.007 (0.004) |
| Caudal anterior cingulate | 2.768 (0.065) | -0.049 (0.086) | **-0.021 (0.006)** | -0.020 (0.008) |
| Caudal middle frontal | 6.249 (0.148) | 0.259 (0.196) | -0.005 (0.009) | -0.005 (0.012) |
| Cuneus | 2.081 (0.06) | -0.029 (0.08) | -0.004 (0.007) | 0.007 (0.009) |
| Entorhinal | 0.689 (0.032) | 0.057 (0.042) | -0.008 (0.005) | -0.008 (0.007) |
| Frontal pole | 0.256 (0.01) | -0.007 (0.014) | **-0.007 (0.001)** | 0.000 (0.002) |
| Fusiform | 5.999 (0.125) | -0.154 (0.166) | **-0.037 (0.011)** | -0.012 (0.015) |
| Inferior parietal | 9.732 (0.215) | -0.563 (0.285) | **-0.062 (0.013)** | -0.008 (0.018) |
| Inferior temporal | 5.671 (0.14) | -0.101 (0.185) | **-0.061 (0.012)** | -0.035 (0.016) |
| Insula | 8.487 (0.144) | -0.032 (0.19) | -0.017 (0.011) | -0.015 (0.014) |
| Isthmus cingulate | 3.654 (0.085) | -0.020 (0.112) | -0.003 (0.007) | -0.012 (0.009) |
| Lateral occipital | 8.091 (0.188) | 0.056 (0.249) | -0.041 (0.025) | 0.044 (0.033) |
| Lateral OFC | 6.178 (0.104) | -0.109 (0.138) | **-0.053 (0.009)** | -0.007 (0.011) |
| Lingual | 4.772 (0.139) | -0.017 (0.183) | 0.008 (0.013) | 0.003 (0.017) |
| Medial OFC | 3.637 (0.11) | 0.027 (0.146) | -0.014 (0.009) | -0.025 (0.011) |
| Middle temporal | 4.826 (0.109) | -0.131 (0.145) | **-0.079 (0.011)** | -0.005 (0.014) |
| Paracentral | 3.559 (0.091) | -0.081 (0.121) | 0.001 (0.01) | 0.014 (0.013) |
| Parahippocampal | 1.494 (0.04) | -0.025 (0.053) | **-0.011 (0.004)** | -0.004 (0.006) |
| Pars opercularis | 3.426 (0.099) | -0.036 (0.132) | **-0.029 (0.005)** | -0.006 (0.007) |
| Pars orbitalis | 0.873 (0.027) | 0.009 (0.036) | **-0.026 (0.004)** | 0.003 (0.006) |
| Pars triangularis | 2.813 (0.096) | -0.070 (0.127) | **-0.035 (0.005)** | 0.005 (0.007) |
| Pericalcarine | 2.928 (0.098) | -0.185 (0.13) | -0.003 (0.007) | 0.010 (0.009) |
| Postcentral | 7.098 (0.159) | -0.071 (0.211) | **-0.037 (0.017)** | 0.010 (0.022) |
| Posterior cingulate | 4.234 (0.083) | -0.197 (0.11) | **-0.035 (0.007)** | -0.010 (0.01) |
| Precentral | 12.815 (0.223) | -0.334 (0.296) | -0.037 (0.022) | 0.039 (0.029) |
| Precuneus | 8.542 (0.185) | -0.261 (0.245) | **-0.026 (0.01)** | -0.004 (0.013) |
| Rostral anterior cingulate | 2.464 (0.063) | 0.041 (0.084) | -0.002 (0.004) | -0.012 (0.006) |
| Rostral middle frontal | 11.291 (0.251) | -0.405 (0.333) | **-0.116 (0.022)** | 0.013 (0.029) |
| Superior frontal | 16.732 (0.325) | -0.606 (0.43) | -0.044 (0.03) | -0.035 (0.04) |
| Superior parietal | 11.536 (0.278) | -0.504 (0.368) | **-0.038 (0.02)** | 0.002 (0.026) |
| Supramarginal | 8.137 (0.196) | -0.380 (0.26) | **-0.060 (0.01)** | 0.002 (0.013) |
| Superior temporal | 7.029 (0.168) | -0.007 (0.222) | **-0.080 (0.012)** | -0.005 (0.015) |
| Temporal pole | 0.669 (0.023) | 0.014 (0.03) | **-0.017 (0.005)** | 0.002 (0.006) |
| Transverse temporal | 0.910 (0.025) | -0.107 (0.033) | 0.000 (0.003) | -0.006 (0.004) |

Notes: bankssts= All values in mL; banks of the superior temporal sulcus; ε4+ = ε4 allele carrier; ε4- = ε4 allele non-carrier; OFC=orbitofrontal cortex; **Bolded** values are statistically significant after controlling for multiple comparisons using false discovery rate

[a] Predicted mean intercept (baseline) of each region. Standard errors of coefficients are in parentheses.

[b] Predicted mean intercept (baseline) of each structure by presence of ε4. Standard errors of coefficients are in parentheses.

[c] Predicted average yearly rate of change (slope). Standard errors of coefficients are in parentheses.

[d] Predicted average yearly rate of change (slope) by presence of ε4. Standard errors of coefficients are in parentheses.

**Table 9:** Coefficients (±SEM) from linear mixed effects of parcellated subcortical Grey Matter regions

| Region | Intercept (baseline) | | Slope (time) | |
| --- | --- | --- | --- | --- |
| | ε4-[a] | ε4+ vs ε4-[b] | ε4-[c] | ε4+ vs ε4-[d] |
| Left Hemisphere | | | | |
| Accumbens | 0.546 (0.019) | 0.000 (0.026) | **-0.015 (0.003)** | 0.002 (0.005) |
| Amygdala | 1.199 (0.032) | -0.021 (0.042) | **-0.023 (0.006)** | 0.014 (0.007) |
| Caudate | 3.596 (0.083) | -0.095 (0.109) | -0.005 (0.006) | -0.008 (0.008) |
| Pallidum | 1.459 (0.032) | 0.011 (0.042) | 0.000 (0.004) | -0.006 (0.005) |
| Putamen | 4.571 (0.108) | -0.042 (0.143) | **-0.046 (0.01)** | -0.005 (0.013) |
| Thalamus | 5.681 (0.096) | -0.040 (0.127) | -0.017 (0.011) | -0.012 (0.015) |
| Right Hemisphere | | | | |
| Accumbens | 0.522 (0.02) | 0.018 (0.026) | 0.003 (0.003) | -0.005 (0.004) |
| Amygdala | 1.398 (0.033) | -0.011 (0.043) | -0.007 (0.006) | -0.006 (0.008) |
| Caudate | 3.712 (0.088) | -0.140 (0.116) | -0.015 (0.009) | 0.005 (0.012) |
| Pallidum | 1.351 (0.033) | -0.010 (0.043) | -0.001 (0.004) | -0.005 (0.005) |
| Putamen | 4.575 (0.092) | 0.034 (0.122) | **-0.030 (0.009)** | -0.016 (0.013) |
| Thalamus | 5.662 (0.094) | 0.023 (0.124) | -0.017 (0.011) | -0.014 (0.015) |

Notes: All values in mL; ε4+ = ε4 allele carrier; ε4- = ε4 allele non-carrier; **Bolded** values are statistically significant after controlling for multiple comparisons using false discovery rate

[a] Predicted mean intercept (baseline) of each region. Standard errors of coefficients are in parentheses.

[b] Predicted mean intercept (baseline) of each structure by presence of ε4. Standard errors of coefficients are in parentheses.

[c] Predicted average yearly rate of change (slope). Standard errors of coefficients are in parentheses.

[d] Predicted average yearly rate of change (slope) by presence of ε4. Standard errors of coefficients are in parentheses.